Advances in Brief

In Vivo Flow Cytometry: A New Method for Enumerating Circulating Cancer Cells

Irene Georgakoudi, Nicolas Solban, John Novak, William L. Rice, Xunbin Wei, Tayyaba Hasan, and Charles P. Lin

Wellman Center for Photomedicine, Massachusetts General Hospital, Harvard Medical School, Boston, Massachusetts

Abstract

The fate of circulating tumor cells is an important determinant of their ability to form distant metastasis. Here, we demonstrate the use of *in vivo* flow cytometry as a powerful new method for detecting quantitatively circulating cancer cells. We specifically examine the circulation kinetics of two prostate cancer cell lines with different metastatic potential in mice and rats. We find that the cell line and the host environment affect the circulation kinetics of prostate cancer cells, with the intrinsic cell line properties determining the initial rate of cell depletion from the circulation and the host affecting cell circulation at later time points.

Introduction

The major prognostic indicator of survival for almost all of the solid tumors is the extent of metastasis that may be determined by the number of circulating tumor cells in the vasculature either as a consequence of a therapeutic intervention or of advanced tumor growth and invasion. For example, in prostate cancer there has been considerable discussion about tumor dissemination after hyperthermia or even diagnostic techniques, such as transurethral resection of the prostate (1, 2). Because of the complex nature of the metastatic process, the relevance of tumor cells in the vasculature to long-term tumor metastasis remains controversial. To understand the relationship between circulating tumor cells and metastasis, earlier studies were performed using radiolabeled or fluorescently labeled tumor cells (3); both approaches are invasive and performed *ex vivo*. A noninvasive technique to quantitatively detect tumor cells in circulation would be valuable because it could provide options for timely interventions and aid in decisions of therapeutic regimens. In this study, we describe an *in vivo* flow cytometry (IVFC) technique and use it to study circulating prostate cancer cells in mice and rats.

Traditional flow cytometry is used routinely to acquire quantitative information about specific cell populations. This method is sensitive and specific; however, one of its drawbacks is that it is invasive, which limits the acquisition of frequent samples from the same animal, and may result in the introduction of artifacts during sample processing. Noninvasive methods, such as positron emission tomography (4), high-resolution magnetic resonance imaging (5), intravital microscopy (6), bioluminescence (7), and confocal and two-photon imaging (8, 9), have been used to visualize different steps along tumor progression and metastasis formation. These techniques span a wide range of spatiotemporal resolutions, and each one is suitable for studying a different aspect of this complex process. However, none of them is optimized to quantitatively detect changes in the number of circulating cells. We recently have described an IVFC technique with the capability to count circulating fluorescently labeled cells in live animals, without the need to extract blood samples (10). The technique allows for continuous monitoring of the circulating cell population of interest, and it yields quantitative results without affecting the physiology of the subject. In the present study, we demonstrate that IVFC can be used to monitor the rapid depletion kinetics of circulating prostate cancer cells and to examine the dependence of circulation kinetics on the cell line and the host environment.

Materials and Methods

Cell Culture. Human prostate LNCaP cells and rat prostate MLL cells, cultured as described previously (11), were transfected with pEGFP-N1 (Clontech, Palo Alto, CA) using Lipofectin reagent (Invitrogen, Carlsbad, CA). Stably transfected populations were obtained by growing the cells in growth media supplemented with 600 μg/ml G418 (Invitrogen). Stable cell lines (LNCaP-GFP and MLL-GFP) were maintained in the same media except that 300 μg/ml G418 (Invitrogen) replaced penicillin/streptomycin. Before injection, suspensions of LNCaP-GFP or MLL-GFP cells were incubated for 30 min at 37°C with 0.1 mM DiD (Molecular Probes, Eugene, OR). Cells then were washed three times, and the cell concentration was adjusted by serial dilution.

Animals. Experiments were carried out on 4–6-week-old male SCID mice and 6–8-week-old male Copenhagen rats. Tail vein injections and IVFC measurements were performed under anesthesia with a 7:1 mixture of ketamine and xylazine. The Committee on Animal Research at the Massachusetts General Hospital approved all of the animal study protocols.

IVFC Measurements. The experimental setup to acquire IVFC measurements has been described in detail previously (10). Briefly, the major veins and arteries of the ear microcirculation were visualized using transillumination with a 520-nm light emitting diode, and an artery ~40 μm in diameter was selected for data acquisition. Light from a HeNe laser was shaped into a slit and imaged across the selected ear artery. Fluorescently labeled cells traversed this slit and were excited one by one as they flowed through the blood vessels of the animal, producing a burst of fluorescence for each cell. A photomultiplier tube detected the fluorescence after appropriate spatial (*i.e.,* confocal slit) and spectral filtering to optimize the sensitivity and specificity of detection.

To assess the depletion kinetics of circulating prostate cancer cells, 10^6 fluorescently labeled cells/20 g body weight were injected through the tail vein, and the animal was placed immediately onto the stage. The first IVFC measurements were acquired within 5–15 min from the time of injection. Additional measurements were acquired at the same vessel location at 1, 2, 4, and at 8 or 10 h, as well as after 1, 2, 3, and 5 days.

Confocal *In vivo* Imaging. Confocal images of circulating DiD-labeled LNCaP cells were acquired at video rate frames using a microscope described previously (12). Fluorescence was excited using a 658-nm diode laser (Microlaser Systems L4–660S-40; Garden Grove, CA) and detected at 695 ± 27.5 nm (Omega, Brattleboro, VT). To label the endothelial cells for visualizing the blood vessel borders, 20 μg of Cy5-conjugated anti-platelet/endothelial cell adhesion molecule monoclonal antibody (Amersham, Piscataway, NJ) were introduced to the circulation of the SCID mouse the day before imaging.

Ex Vivo Imaging. To assess the level of arrest of the injected prostate cancer cells in various organs, one to two mice and rats were sacrificed at 2 and 24 h postinjection. Lungs, liver, spleen, kidneys, and a small number of lymph nodes were harvested and examined under a standard fluorescence microscope using a 10× objective to visualize arrested GFP-expressing LNCaP or MLL cells.

Results and Discussion

Imaging and Enumerating Circulating Cells *In vivo*. Circulating DiD-fluorescently labeled cells can be readily visualized flowing through the ear microcirculation using video-rate confocal microscopy (Fig. 1*A* and Supplemental video). The use of confocal imaging is not optimal to enumerate circulating cells because that would require sophisticated image-processing algorithms. In addition, arterial flow often is so fast as to cause image blurring even at video rate acquisition. For these reasons, the newly developed IVFC is a simple and potentially far more powerful method to enumerate circulating cells. Fig. 1*B* shows a representative data trace, in which individual fluorescence peaks correspond to single cells that are excited as they traverse the laser slit of the IVFC. A control trace acquired from the same mouse artery before injection of fluorescently labeled cells also is included. The intensity of the recorded peaks varies, probably because of corresponding variations in the intensity of fluorescence staining of individual cells. The corresponding scatter plot, including the peak height and the full width at half maximum of each detected peak, is shown in Fig. 1*C*. The full width at half maximum is associated with the *in vivo* flow velocity of the corresponding cell because it represents the amount of time required to cross the excitation slit of light, which is ~5 μm across.

To assess whether the number of cells detected immediately after inoculation depends on the number of inoculated cells and to estimate how many circulating cells are needed to detect a few cells within a reasonable amount of monitoring time, we injected different numbers of LNCaP cells, varying from 10^3 to 10^6, and performed IVFC measurements immediately following injection. These measurements illustrate that with only 1000 cells in the circulation, we can detect unambiguously and reproducibly a few cells in a 10-min recording period (Fig. 1*D*). The absolute number of detected cells per minute may vary from experiment to experiment. This could be the result of errors in estimating the cell concentration of the inoculum and variability in the number of cells successfully introduced in the mouse circulation. Small variations in the size of the selected arteries and in the flow velocity of cells also can affect the absolute number of detected cells. Nevertheless, a clear relationship is observed between the number of injected and the number of detected cells/min. Potentially <1000 cells can be detected in the circulation by selecting larger arteries for measurements.

Circulation Kinetics of Prostate Cancer Cells in Mice and Rats. The number of detected cells/min as a function of time following injection of fluorescently labeled LNCaP and MLL prostate cancer cells in mice and in rats is shown in Fig. 2. All of the measurements are normalized to the number of cells detected immediately after cell injection. Individual traces report the numbers acquired from individual animals, and each time point is represented by the mean and SD of the number of cells detected during a period of at least 6 min. However, in the case of the MLL studies, there was a significant and systematic decrease in the number of cells detected during the initial recorded intervals. Therefore, these numbers are reported without a corresponding SD because they represent a single 1-min measurement.

Typically, >80–90% of both cell types are depleted from the circulation of mice and rats within the first 2–4 h. Interestingly, the number of the more highly metastatic MLL cells decreases at a significantly faster rate than that of the LNCaP cells. The depletion of LNCaP and MLL cells follows a systematic pattern that is reproducible among different SCID mice (Fig. 2*A*). Once the initial depletion takes place, the number of circulating prostate cancer cells remains consistently low during a period of days (Fig. 2*B*).

MLL cells also become depleted faster than LNCaP cells in the circulation of Copenhagen rats, even though we see greater variability in the detected number of cells (Fig. 2, *C* and *D*). The initial rate of depletion of LNCaP cells in the two different hosts is similar. MLL cells also become depleted at similar rates from the circulation of mice and rats. However, in all of the MLL-injected rats and in two of the three LNCaP-injected rats, we observe an increase in the number of circulating cells following this initial depletion. In the LNCaP case, this increase is observed either at the 2- or 4-h time point and is followed by a significant decrease by the time of the following set of measure-

Fig. 1. *A,* combined image of three still frames, spanning 200 ms, from a movie acquired at video rate (included as a Supplemental video) showing DiD-labeled MLL cells traveling through an artery vein pair. Two cells are highlighted along the vein (*top vessel*) and one cell along the artery (*bottom vessel*) using blue, green, and red for the same cells as they are imaged in the first, second, and third frames, respectively. To help visualize the blood vessels, the vascular endothelium is labeled simultaneously with anti-platelet/endothelial cell adhesion molecule-1 (CD31) conjugated to Cy5. *B,* representative signal trace recorded from an ear artery of a SCID mouse injected with 10^6 DiD-labeled MLL cells. Each spike is created by the fluorescence burst resulting from an MLL cell traversing the excitation slit. Corresponding control trace is shown in red. Individual fluorescence peaks are shown in more detail in the inset. *C,* scatter plot illustrating the distribution in the height and width of the detected fluorescence peaks from the control trace (*red*) and the trace acquired following injection of MLL DiD-labeled cells (*blue*). *D,* the number of detected cell counts/min is highly correlated to the number of injected cells. Consistent cell counts/min are acquired with *in vivo* flow cytometry even when as few as 1000 cells are injected in the SCID mouse circulation.
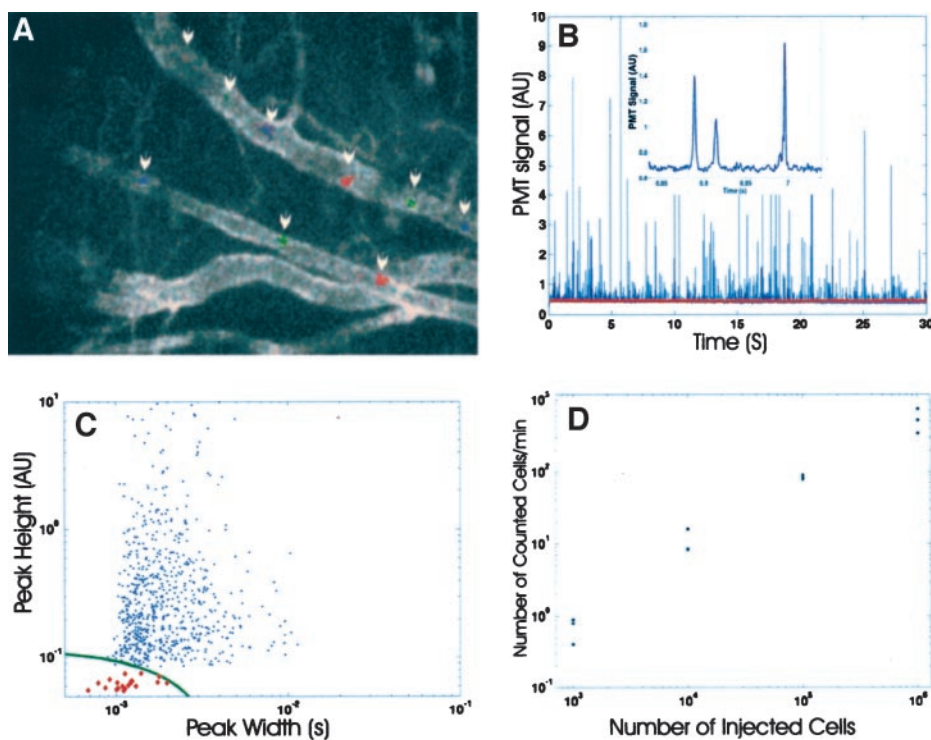

5045

Fig. 2. Depletion kinetics of circulating LNCaP (*black lines*) and MLL (*gray lines*) cells in SCID mice (*solid lines*, *A* and *B*) and Copenhagen rats (*dashed lines*, *C* and *D*). The normalized numbers of circulating cells/min are shown for the first 10 h following injection of the fluorescently labeled cells (*A* and *C*) to illustrate the differences observed in the initial depletion rate of LNCaP and MLL cells. Data from the same set of animals during the course of several days are included in *B* and *D*, demonstrating differences in the circulation kinetics of these cancer cells in SCID mice and rats.
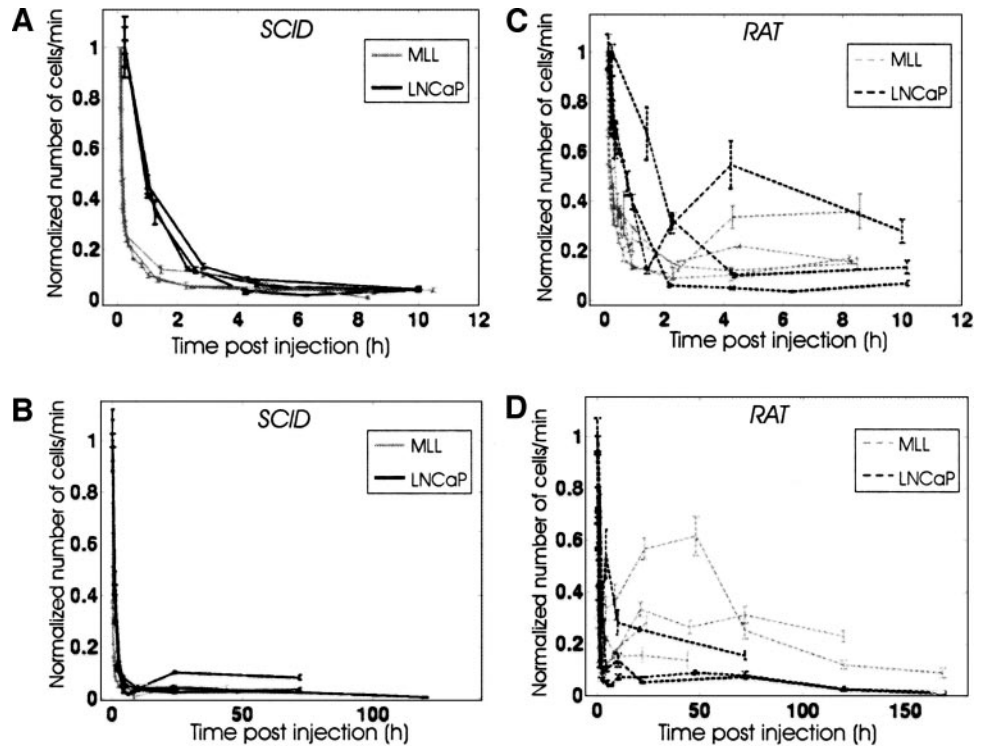
ments. In the MLL case, this reappearance of circulating cells persists typically for several days and is followed by a slow redepletion.

These results are consistent with those reported by Fidler *et al.* (13), who used ^{125}I-5-iodo-2′-deoxyuridine-labeled melanoma cells and showed they become rapidly depleted from the circulation. They also observed a reappearance and redepletion of cancer cells, even though the kinetics of this behavior were different from our study, probably because of differences in the intrinsic properties of the examined cell lines and the host.

Histograms representing the normalized distributions of fluorescence peak heights and full widths at half maximum of circulating LNCaP cells are included in Fig. 3. Each panel represents information acquired from at least three animals at each of the three different time points. Whereas the absolute number of cells detected immediately after and at 2 and 24 h following injection is different, the detected fluorescence peak characteristics are similar. The largest number of peaks ranges in width between 0.001–0.003 s, corresponding to a flow velocity of 2.3–7 mm/s, consistent with expected results (14). The fact that the peak height distribution of the circulating cells does not change with time suggests that there are no significant changes in the level of cell labeling. Similar results were acquired with the MLL cell studies.

***Ex Vivo* Imaging of Arrested Prostate Cancer Cells.** *Ex vivo* imaging of several organs 2 h following injection of GFP-transfected LNCaP and MLL cells reveals that a significantly higher number of the more highly metastatic MLL cells are retained in the lung compared with LNCaP cells, which may explain the differences in the initial depletion rates from the circulation detected by IVFC (Fig. 4, *A* and *B*). Interestingly, at 24 h postinjection, we continue to detect a significant number of MLL cells in the lung but no LNCaP cells (Fig. 4, *C* and *D*). This suggests that LNCaP cells become initially arrested in the lung, but then a significant fraction of this population undergoes apoptosis or necrosis. This behavior is consistent with previous studies demonstrating an inverse correlation between the levels of *in vivo* apoptosis and metastatic potential (15). No significant fluorescence

was detected in any of the other examined organs. However, because we did not examine all of the lymph nodes, it is possible that some cells are arrested there.

Several studies have examined the mechanisms responsible for the metastasis of tumor cells. In some cases, cells become physically trapped in the microcirculation of certain organs, such as the lungs or the liver, because of their size (16, 17). This probably is not the main reason for which MLL cells are arrested in the lung in higher numbers than LNCaP cells because MLL cells in suspension are smaller (17.6 ± 3.8 μm) than LNCaP cells (23 ± 4.8 μm). In other cases, the expression of specific adhesion molecules, such as P-selectin and
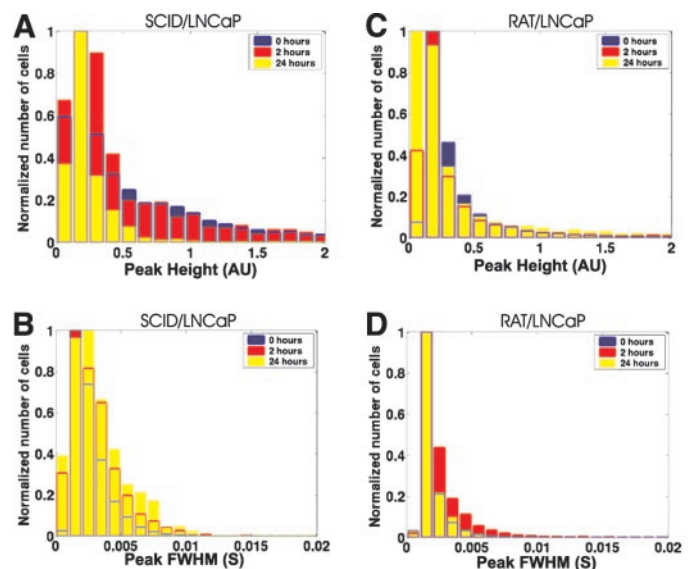

Fig. 3. Similar fluorescence peak height (*A* and *C*) and width (*B* and *D*) distributions are observed for LNCaP cells circulating in mice (*A* and *B*) and rats (*C* and *D*). These distributions generally are similar for the peaks detected at different time points following cancer cell injection, even though the number of detected cells varies significantly.
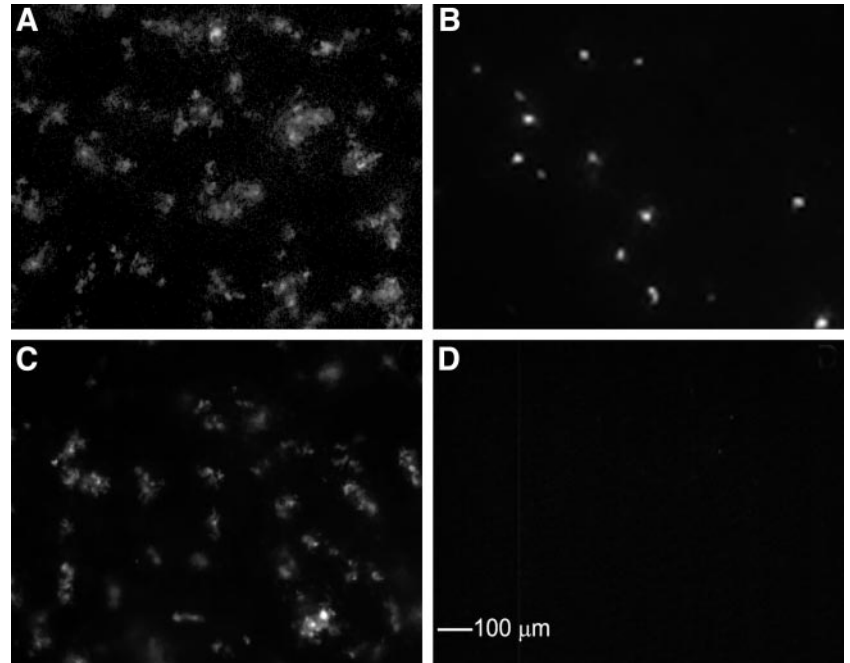
5046

Fig. 4. A higher number of MLL (*A*) than LNCaP (*B*) cells are seen trapped in the lungs of SCID mice 2 h following tail vein injection. This trend persists at 24 h postinjection with virtually no fluorescence detected in the lungs of the SCID mouse injected with LNCaP cells (*D*), whereas significant levels of fluorescence persist in the case of the MLL cells (*C*).

fibrinogen, is responsible for the homing of cancer cells to an organ (17, 18). Changes in the expression levels of such molecules could explain the reappearance of cancer cells in the rat circulation because cancer cells may remain in the intravascular lung space and form tumors before extravasation (19).

In summary, we demonstrate that IVFC is a promising new tool to enumerate cells in circulation, which can help us to address some important questions regarding the relationship of circulating cancer cells to metastasis and long-term cancer survival and to monitor response to specific treatment modalities.

Acknowledgments

References

1. Lein M, Koenig F, Misdraji J, et al. Laser-induced hyperthermia in rat prostate cancer: role of site of tumor implantation. Urology 2000;56:167–72.
2. Siddiqua A, Chendil D, Rowland R, et al. Increased expression of PSA mRNA during brachytherapy in peripheral blood of patients with prostate cancer. Urology 2002;60: 270–5.
3. Fidler I. The pathogenesis of cancer metastasis: the "seed and soil" hypothesis revisited. Nat Rev Cancer 2003;3:453–8.
4. Dubey P, Su H, Adonai N, et al. Quantitative imaging of the T cell antitumor response by positron-emission tomography. Proc Natl Acad Sci USA 2003;100:1232–7.
5. Dodd SJ, Williams M, Suhan JP, Williams DS, Koretsky AP, Ho C. Detection of single mammalian cells by high-resolution magnetic resonance imaging. Biophys J 1999;76:103–9.
6. Naumov GN, Wilson SM, MacDonald IC, et al. Cellular expression of green fluorescent protein, coupled with high-resolution in vivo videomicroscopy, to monitor steps in tumor metastasis. J Cell Sci 1999;112:1835–42.
7. Sweeney TJ, Mailander V, Tucker AA, et al. Visualizing the kinetics of tumor-cell clearance in living animals. Proc Natl Acad Sci USA 1999;96:12044–9.
8. Wang W, Wyckoff JB, Frohlich VC, et al. Single cell behavior in metastatic primary mammary tumors correlated with gene expression patterns revealed by molecular profiling. Cancer Res 2002;62:6278–88.
9. Padera TP, Kadambi A, di Tomaso E, et al. Lymphatic metastasis in the absence of functional intratumor lymphatics. Science 2002;296:1883–6.
10. Novak J, Georgakoudi I, Wei X, Prossin A, Lin CP. In vivo flow cytometer for real-time detection and quantification of circulating cells. Opt Lett 2004;29:77–9.
11. Momma T, Hamblin MR, Wu HC, Hasan T. Photodynamic therapy of orthotopic prostate cancer with benzoporphyrin derivative: local control and distant metastasis. Cancer Res 1998;58:5425–31.
12. Rajadhyaksha M, Anderson R, Webb R. Video-rate confocal scanning laser microscope for imaging human tissues in vivo. Appl Opt 1999;38:2105–15.
13. Fidler I. Metastasis: quantitative analysis of distribution and fate of tumor emboli labeled with ^{125}I-5-Iodo-2′-deoxyuridine. J Natl Cancer Inst 1970;45:773–82.
14. Chen Z, Milner T, Srinivas S, et al. Noninvasive imaging of in vivo blood flow velocity using optical Doppler tomography. Opt Lett 1997;22:1119–21.
15. Wong CW, Lee A, Shientag L, et al. Apoptosis: an early event in metastatic inefficiency. Cancer Res 2001;61:333–8.
16. Zeidman I, McCutcheon M, Coman D. Factors affecting the number of tumor metastases experiments with a transplantable mouse tumor. Cancer Res 1950;10: 357–9.
17. Ding L, Sunamura M, Kodama T, et al. In vivo evaluation of the early events associated with liver metastasis of circulating cancer cells. Br J Cancer 2001;85: 431–8.
18. Palumbo JS, Kombrinck KW, Drew AF, et al. Fibrinogen is an important determinant of the metastatic potential of circulating tumor cells. Blood 2000;96:3302–9.
19. Al-Mehdi AB, Tozawa K, Fisher AB, Shientag L, Lee A, Muschel RJ. Intravascular origin of metastasis from the proliferation of endothelium-attached tumor cells: a new model for metastasis. Nat Med 2000;6:100–2.

In Vivo Flow Cytometry: A New Method for Enumerating Circulating Cancer Cells

Irene Georgakoudi, Nicolas Solban, John Novak, et al.

Updated version	Access the most recent version of this article at: http://cancerres.aacrjournals.org/content/64/15/5044
Supplementary Material	Access the most recent supplemental material at: http://cancerres.aacrjournals.org/content/suppl/2004/08/24/64.15.5044.DC1

Cited articles	This article cites 19 articles, 9 of which you can access for free at: http://cancerres.aacrjournals.org/content/64/15/5044.full#ref-list-1
Citing articles	This article has been cited by 13 HighWire-hosted articles. Access the articles at: http://cancerres.aacrjournals.org/content/64/15/5044.full#related-urls

E-mail alerts	Sign up to receive free email-alerts related to this article or journal.
Reprints and Subscriptions	To order reprints of this article or to subscribe to the journal, contact the AACR Publications Department at pubs@aacr.org.
Permissions	To request permission to re-use all or part of this article, use this link http://cancerres.aacrjournals.org/content/64/15/5044. Click on "Request Permissions" which will take you to the Copyright Clearance Center's (CCC) Rightslink site.